Long-haul DWDM transmission systems employing optical phase conjugation

Long-Haul DWDM Transmission Systems Employing Optical Phase Conjugation

S. L. Jansen, *Student Member, IEEE*, D. van den Borne, *Student Member, IEEE*, P. M. Krummrich, *Member, IEEE*, S. Spälter, G.-D. Khoe, *Fellow, IEEE*, and H. de Waardt

(Invited Paper)

***Abstract*—In this paper, we review the recent progress in transmission experiments by employing optical phase conjugation (OPC) for the compensation of chromatic dispersion and nonlinear impairments. OPC is realized with difference frequency generation (DFG) in a periodically poled lithium-niobate (PPLN) waveguide, for transparent wavelength-division multiplexed (WDM) operation with high conversion efficiency. We discuss extensively the principle behind optical phase conjugation and the realization of a polarization independent OPC subsystem. Using OPC for chromatic dispersion compensation WDM 40-Gb/s long-haul transmission is described. As well, transmission employing both mixed data rates and mixed modulation formats is discussed. No significant nonlinear impairments are observed from the nonperiodic dispersion map used in these experiments. The compensation of intrachannel nonlinear impairments by OPC is described for WDM carrier-suppressed return-to-zero (CSRZ) transmission. In this experiment, a 50% increase in transmission reach is obtained by adding an OPC unit to a transmission line using dispersion compensating fiber (DCF) for dispersion compensation. Furthermore, the compensation of impairments due to nonlinear phase noise is reviewed. An in-depth analysis is conducted on what performance improvement is to be expected for various OPC configurations and a proof-of-principle experiment is described showing over 4-dB improvement in Q-factor due to compensation of nonlinear impairments resulting from nonlinear phase noise. Finally, an ultralong-haul WDM transmission of 22×20-Gb/s return-to-zero differential quadrature phase-shift keying (RZ-DQPSK) is discussed showing that OPC can compensate for chromatic dispersion, as well as self-phase modulation (SPM) induced nonlinear impairments, such as nonlinear phase noise. Compared to a "conventional" transmission link using DCF for dispersion compensation, a 44% increase in transmission reach is obtained when OPC is employed. In this experiment, we show the feasibility of using only one polarization-independent PPLN subsystem to compensate for an accumulated chromatic dispersion of over 160 000 ps/nm.**

***Index Terms*—Dispersion compensation, differential phase-shift keying (DPSK), differential quadrature phase-shift keying (DQPSK), duobinary, fiber-optics communications, nonlinear phase noise, phase conjugation, phase-shift keying, periodically poled lithium niobate (PPLN), spectral inversion.**

Manuscript received August 16, 2005; revised March 10, 2006. This work was supported in part by in part by Eindhoven University of Technology, Eindhoven, The Netherlands, and Siemens AG, Munich, Germany.

S. L. Jansen, D. van den Borne, G.-D. Khoe, and H. de Waardt are with the COBRA Institute, Eindhoven University of Technology, 5600 MB Eindhoven, The Netherlands (e-mail: s.l.jansen@tue.nl; d.v.d.borne@tue.nl; g.d.khoe@tue.nl; h.d.waardt@tue.nl).

P. M. Krummrich and S. Spälter are with the Siemens AG, D-81359 Munich, Germany (e-mail: peter.krummrich@siemens.com; stefan.spaelter@siemens.com).

Digital Object Identifier 10.1109/JSTQE.2006.876621

I. Introduction

OPTICAL phase conjugation (OPC), sometimes referred to as spectral inversion, is a promising technology to compensate for deterministic impairments in long-haul transmission systems such as Kerr nonlinearities and chromatic dispersion. By optically conjugating the phase of the signal in the middle of the link, impairments that occurred in the first part of the transmission link (before conjugation) can be cancelled by impairments that occur in the second part of the link (after conjugation).

Initially, chromatic dispersion compensation by OPC was proposed by Yariv *et al.* in 1979 [1]. In such a transmission link, the inline dispersion compensating fiber (DCF) modules are omitted, saving the extra insertion loss of the DCF modules, which can result in a higher optical signal-to-noise ratio (OSNR) after transmission for an equivalent transmission line. As well, a simplified design of the inline dispersion map and inline amplifiers is realized through midlink OPC, since the chromatic dispersion accumulates along the transmission line, resulting effectively in the absence of a periodic inline dispersion map. Apart from the compensation for chromatic dispersion, OPC can be employed to cancel nonlinear impairments resulting from the Kerr effect such as self phase modulation (SPM) [2], [3], intrachannel nonlinear effects [4]–[7] and nonlinear phase noise [8], [9].

In this work, recent developments in long-haul transmission by employing OPC are discussed. Most recent OPC transmission experiments have been conducted using a periodically poled lithium-niobate (PPLN) waveguide for OPC. In Section II, the PPLN waveguide used to realize OPC is discussed. We analyze OPC from a theoretical point of view in Section III. An overview of transmission experiments employing OPC is given in Section III, as well. OPC for chromatic dispersion compensation is discussed in Section IV, showing wavelength-division multiplexed (WDM) 40 Gb/s and modulation format transparent transmission without inline dispersion compensation. Section V covers two experiments showing that OPC can compensate for impairments due to intrachannel nonlinear effects as well as nonlinear phase noise. An ultralong-haul 20-Gb/s differential quadrature phase-shift-keying (DQPSK) transmission experiment will be described in Section VI, using OPC for compensation of chromatic dispersion, as well as SPM induced nonlinear impairments, such as nonlinear phase noise. The performance of the OPC-based transmission is compared to "conventional" optimized DCF-based transmission. A 44% increase in transmission

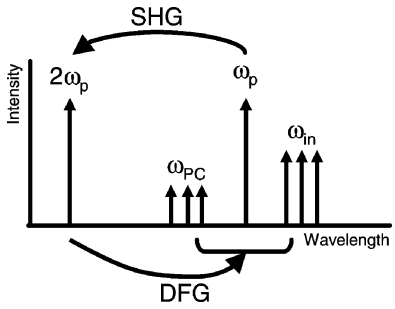

Fig. 1. Principles of SHG and DFG.

reach is reported. Section VII provides an outlook for OPC in long-haul transmission, and Section VIII summarizes the paper.

II. Periodically Poled Lithium Niobate

Several techniques have been proposed to phase conjugate an optical signal. Most of the realized OPC units are based on the following processes: Four-wave mixing (FWM) in a highly nonlinear fiber (HNLF), FWM in a semiconductor optical amplifier (SOA) or parametric difference frequency generation (DFG) in a PPLN waveguide. The first OPC transmission experiments were based on FWM in either a HNLF or SOA [10]–[20]. Using HNLF for OPC, high conversion efficiencies of up to $\sim$0 dB have been reported [20]. However, both HNLF and SOAs suffer from third-order nonlinear impairments such as SPM and cross-phase modulation (XPM) in the phase conjugation process. Additionally in SOAs intrinsic noise in the form of amplified spontaneous emission (ASE) is generated. DFG in a PPLN waveguide has been used in most recent transmission experiments, and therefore, we focus on this technique. In this section, several advantages and disadvantages of the PPLN waveguide for OPC are discussed.

A. PPLN Waveguide for OPC

Phase conjugation with a PPLN waveguide is realized by second harmonic generation (SHG) and DFG. Both DFG and SHG are based on the second-order nonlinear susceptibility (χ^2) [21], [22], rather than third-order susceptibility (χ^3) that is well known for causing impairments in optical transmission. The principle of the cascaded SHG and DFG process is illustrated in Fig. 1. Through SHG, the pump at frequency $\omega_{\rm p}$ is up converted to the frequency $2\ \omega_{\rm p}$. Simultaneously, DFG occurs where the second harmonic $(2\omega_{\rm p})$ interacts with N input signals, at frequencies $\omega_{1\_{\rm in}}$ to $\omega_{{\rm n}\_{\rm in}}$, to generate phase-conjugated signals at the frequencies $\omega_{1\_{\rm PC}} = 2\omega_{\rm p} - \omega_1$ to $\omega_{{\rm N}\_{\rm PC}} = 2\omega_{\rm p} - \omega_{N\_in}$.

For efficient nonlinear interactions (SHG and DFG) between the pump and the signals inside the PPLN waveguide, the phase mismatch caused by dispersion of the lithium-niobate needs to be compensated for. This dispersion can be compensated for by quasi-phase matching (QPM). First-order QPM can be realized by reversing the sign of the nonlinear susceptibility (periodically poling) with every phase matching period. Typically, the phase matching period of the periodic poling is $\sim$16.5 μm and this determines the wavelength of the pump signal. Exact tuning of the phase matching can be realized by setting the operating temperature of the OPC unit. A concern of OPC through a PPLN waveguide is that it suffers from the presence of the photorefractive effect. The photorefractive effect can be mitigated by heating the waveguide. Typically, a PPLN waveguide is operated at 180–200 °C. Because of the high operating temperature, picktail fibers cannot be glued to the waveguide with generally available techniques and-hence-free-space optics has to be used to couple the light in and out of the waveguide.

Several waveguides have been developed where the photorefractive effect is reduced, such as the annealed proton exchanged (APE) PPLN or the magnesium-oxide (MgO)-doped PPLN [23], [24]. These waveguides can be operated at significantly lower temperatures. In several recent transmission experiments APE [4]–[7], [25], [26] and MgO-doped [27]–[32] PPLN waveguides are employed operating at temperatures ranging from 50 °C to 90 °C. The lower operating temperature allows gluing the fibers to the waveguide and therefore the MgO-doped PPLN waveguides are more practical for subsystem integration.

The cascaded DFG process in a PPLN waveguide mimics FWM, which is a χ^3 process. However, real χ^3 processes such as SPM, XPM, and FWM are small inside the PPLN waveguide and can be neglected; hence, no signal distortions are introduced in the converted signal. An advantage of the cascaded DFG process is that it is instantaneous and phase sensitive in its response, the OPC through a PPLN waveguide is therefore transparent to data rate and modulation format. Other advantages of the PPLN waveguide are that negligible noise is added to the phase-conjugated signal and that it allows for high conversion efficiencies [33].

The PPLN waveguide has a broadband conversion bandwidth (typically > 50 nm) and is therefore, capable of conjugating multiple WDM channels with one single unit. Simultaneous phase conjugation of up to 103×10 Gb/s has been demonstrated by Yamawaku *et al.* [34]. In this 10-Gb/s nonreturn-to-zero (NRZ) experiment, 103 channels in the C-band (1531–1551 nm), are optically phase conjugated with one PPLN waveguide to the L-band (1559–1579 nm) with a conversion efficiency of about -15 dB. At the output of the PPLN waveguide, the phase-conjugated channels are present mirrored with respect to the pump signal. In this experiment, the pump signal is present at 1555 nm. The optical spectrum after the PPLN waveguide is depicted in Fig. 2.

B. Polarization Diversity

A concern with OPC is that a PPLN waveguide is intrinsically polarization dependent. In a transmission system, signals have an arbitrary polarization that both is different for each WDM channel and can change quickly over time. Hence, a polarization-independent OPC unit is required. Here, two polarization diversity schemes will be discussed: the parallel [35] and the counter-directional [36] polarization diversity structure.

The parallel polarization diversity structure is depicted in Fig. 3. The signal (at random polarization) is combined with a pump signal and fed into a polarization beam splitter (PBS). After the PBS, in both arms of the parallel structure, a PPLN

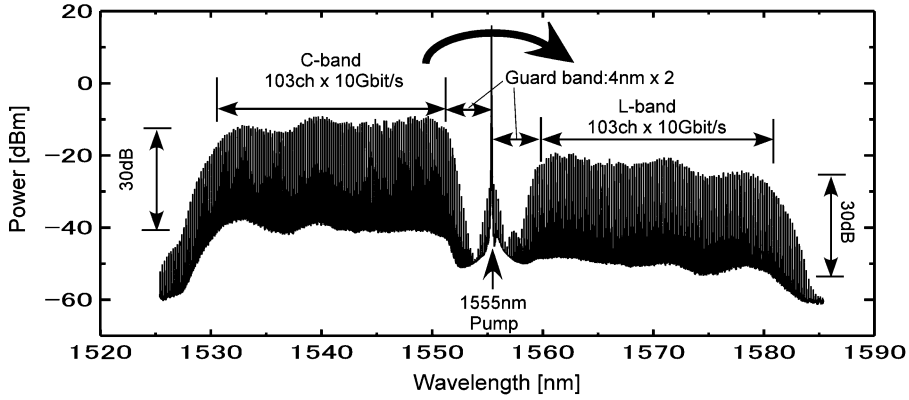

Fig. 2. Output spectrum of the PPLN waveguide. Conversion of 103 × 10-Gb/s NRZ from the C-band to the L-band [34].

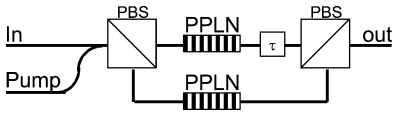

Fig. 3. Parallel polarization-independent OPC unit.

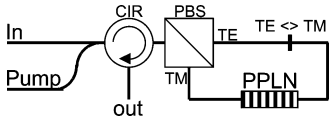

Fig. 4. Counterdirectional polarization-independent OPC unit.

waveguides is present. The two waveguides must be nearly identical with the same conversion efficiency and periodic poling. This can for example be realized by using two waveguides of a single PPLN crystal. The output ports of the PBS are polarization maintaining fibers and aligned such that the PPLN waveguides receive the data and pump signal in the TM polarization. After phase conjugation, the signal is recombined by a second PBS. In one of the arms of the polarization diversity structure, a delay line is present which is used to equalize the length of both arms. This delay line must be precisely set on the bit level, since unequal lengths of the arms of the parallel structure would result in differential group delay (DGD). The pump wavelength is launched at 45 ° with respect to the principal axes of the first PBS such that both PPLN waveguides receive the same amount of optical pump power. Alternatively, the pump signal can be added in each arm of the parallel structure. In this case, each PPLN waveguide can receive 3 dB more pump power. However, two pump signals are required in this case instead of one. The parallel polarization diversity-based OPC unit was initially introduced using FWM in two SOAs [12] and afterwards adapted for conversion using two PPLN waveguides [35].

The counter-directional OPC structure is realized by using both directions of propagation in a single PPLN waveguide [36]. The layout of the counter-directional OPC structure is depicted in Fig. 4. A PBS splits the incoming signal into TE and TM mode. The TM mode is phase conjugated in the PPLN waveguide and subsequently converted to TE mode by aligning the TE with the TM mode in a splice. The TE mode is first converted from the TE to the TM mode and afterwards phase conjugated. Both counter-propagating modes are recombined at the first PBS to effectively provide polarization-independent phase conjugation. The pump signal is added before the data signal enters the polarization diversity structure. In order to pump both directions of the PPLN waveguide, the pump is launched at 45 ° with respect to the principal axes of the PBS such that the pump is split in a 50%–50% ratio.

The main advantages of the counter-directional OPC structure over the parallel structure are that only one PPLN waveguide is required and that both parts of the data (TE and TM modes) travel through the same components. As a result, both parts of the signal will arrive at the PBS at the same time. Hence, the counter-directional OPC unit has inherently low DGD and PDL. A disadvantage, however, is that this scheme can be impaired by multiple path interference when the extinction ratio of the PBS is too low.

III. Phase Conjugation in Optical Transmission

A. Theory of Phase Conjugation

The propagation of a signal in a nonlinear, dispersive and lossy medium can be expressed by the nonlinear Schrödinger equation assuming a slowly varying envelope approximation [37]

$$\frac{\partial A}{\partial z} = -\frac{\alpha}{2}A - \frac{i}{2}\beta_2\frac{\partial^2 A}{\partial T^2} + \frac{1}{6}\beta_3\frac{\partial^3 A}{\partial T^3} + i\gamma|A|^2 A \quad (1)$$

where A represents the complex amplitude of the signal, z the propagation distance in km, α the attenuation coefficient in neper per kilometer, γ the nonlinearity coefficient (Kerr effect) in 1/(W·km), and $T = t - z/v_g$ the time measured in a retarded frame. β_2 in ps^2/nm and β_3 in ps^3/nm are terms for the group-velocity dispersion (GVD) and dispersion slope, respectively. Its complex conjugate can be expressed as

$$\frac{\partial A^*}{\partial z} = -\frac{\alpha}{2}A^* + \frac{i}{2}\beta_2\frac{\partial^2 A^*}{\partial T^2} + \frac{1}{6}\beta_3\frac{\partial^3 A^*}{\partial T^3} - i\gamma|A^*|^2 A^* \quad (2)$$

where $*$ denotes the complex-conjugate operation. Note that in this equation the signal evolution over the fiber after conjugation is still denoted by A. In this expression, it can be seen that the sign of the chromatic dispersion term (β_2) and the Kerr effect term (γ) are both inverted. The chirp induced through GVD

increases linear along the transmission link. Since the sign of the GVD term is inverted by OPC, the GVD induced chirp that occurs after OPC cancels the GVD induced chirp before OPC. Thus, in a transmission link with the same fiber before and after OPC, full GVD compensation is obtained by placing the OPC midlink.

The compensation of the Kerr effect is analog to that of the GVD. However, the Kerr effect is unlike the GVD, a nonlinear impairment, dependent on the optical power of the signal. As a result, the degree in which the Kerr effect is compensated for is dependent on the design of the transmission link.

Using (1) and (2), Watanabe and Shirasaki presented in [2] a general condition for perfect compensation of the Kerr effect term by making the fiber parameters α, β_2, and γ dependent on the transmission distance z. Neglecting the third-order dispersion, this results in

$$\frac{\beta_2(-z_1)}{\gamma(-z_1)P(-z_1)} = \frac{\beta_2(z_2)}{\gamma(z_2)P(z_2)} \tag{3}$$

where the OPC unit is present at $z = 0$, $-z_1$ is the transmission distance before the OPC unit, and z_2 is the transmission distance after the OPC unit. $P(z)$ in Watt is the optical power at point z. Basically, the Kerr effect can be totally compensated for when the ratio of nonlinear effects (γP) to chromatic dispersion (β_2) is equal at $-z_1$ and z_2. In such a transmission line, OPC is capable of compensating both chromatic dispersion and nonlinear impairments.

The signs of the attenuation term (α) and the dispersion slope term (β_3) remain unchanged before and after OPC. Therefore, these impairments cannot be compensated for through OPC. An effect of the dispersion slope is that the GVD is different for each wavelength. With OPC, a wavelength conversion occurs and therefore the GVD before and after OPC is different for the WDM channels. As a result, a difference in residual dispersion is present after transmission. In most OPC-based transmission experiments reported so far, the difference in residual dispersion is compensated for by optimizing the postcompensation after transmission on a per channel basis [15], [16], [25], [27]–[32], [39], [40]. Alternatively, the third-order dispersion can be compensated for using a slope compensator [38].

Apart from the dispersion slope and the attenuations, the most significant impairment that fundamentally cannot be compensated for by OPC is polarization mode dispersion (PMD). Most notably because PMD is a statistical impairment, as a result the amount of PMD in the link changes with time and is not symmetrically distributed along the transmission line.

B. Transmission Line Symmetry

An important consideration of (3) is that total compensation of chromatic dispersion and the Kerr effect can only be realized in a perfectly symmetric transmission link with respect to $\beta_2(z), \gamma(z)$, and $P(z)$. However, due to the attenuation of the optical fiber, the power envelope along the transmission line is nonconstant. This complicates realizing a power symmetric transmission line with respect to the OPC unit.

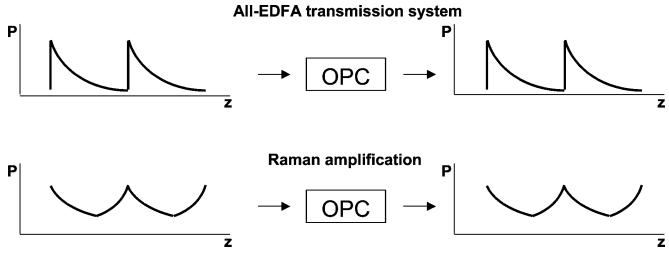

Fig. 5. Power envelope along the transmission line for an EDFA-amplified and a Raman-amplified transmission system.

In Fig. 5, the power envelope along the transmission line is depicted for a "conventional" erbium-doped fiber-amplified (EDFA) and a Raman-amplified transmission line. In the "conventional" EDFA-amplified system, the power envelope with respect to the OPC unit is asymmetric, which reduces the amount of Kerr effect that can be compensated for. This problem can be circumvented by using Raman amplification and thereby create a more symmetric power envelope along the transmission line [26]. However, a disadvantage of all-Raman amplification is that it is a complicated solution that requires high pump powers. Chowdhury *et al*. showed that also with a hybrid EDFA/Raman amplification scheme, where the power is not symmetric with respect to the OPC unit, significant nonlinearity compensation can be achieved [4]–[7].

C. OPC-Aided Transmission

Since the introduction of OPC for chromatic dispersion compensation in 1979 [1], OPC-based transmission has attracted significant research interest. Table I provides an overview of some OPC-based multispan transmission experiments. Transmission experiments with OPC were first conducted in 1993, using FWM in dispersion-shifted fiber (DSF) for OPC. Multispan transmission experiments were reported at both 2.5 [10] and 10 Gb/s [11] over 400 km of standard single-mode fiber (SSMF). Watanabe *et al*. showed that one 20-Gb/s OTDM channel can be transmitted over 3000-km DSF [12]. DSF is, however, not an optimal fiber for WDM transmission due to high FWM impairments. SSMF, the most common fiber deployed today was used in [13]. In this multispan transmission experiment 40 Gb/s was transmitted over 406 km, using FWM in an SOA for OPC. In these experiments, a polarization-dependent OPC was used and the polarization of the data signal was aligned to obtain maximum conversion efficiency. The transmission of 40 Gb/s over 434 km, using a polarization-independent OPC was first reported in [14].

The experiments mentioned above are all single channel. WDM transmission over 100 km of fiber has been shown at 10 [15] and 40 Gb/s [16]. The first multispan WDM experiment was published in [20] transmitting five channels 10 Gb/s over 320 km of SSMF. In this experiment, FWM in HNLF was used for OPC. With a PPLN waveguide as the OPC medium, the transmission reach was increased to 990 km, transmitting five channels at 10 Gb/s with a 100-GHz spacing [27]. By reducing the channel spacing to 50 and 25 GHz, the performance of OPC-based transmission was tested in an XPM-limited environment

TABLE I
MULTISPAN TRANSMISSION EXPERIMENTS EMPLOYING OPTICAL PHASE CONJUGATION

# of Ch, spacing	Data rate mod Form	Distance (km)	Fiber type	Spans (km)	OPC-medium	Ref.
1ch	2.5Gbit/s	400	SSMF	80	DSF	1993, [10]
1ch	10Gbit/s NRZ	400	SSMF	80	DSF	1993, [11]
1ch	20Gbit/s RZ	3,000	DSF	66	DSF	1995, [12]
1ch	40Gbit/s RZ	406	SSMF	~101.5	SOA	1997, [13]
1ch	40Gbit/s RZ	434	SSMF	~108.5	SOA	1998, [14]
5ch, 200GHz	10Gbit/s RZ	320	SSMF	80	HNLF	2003, [20]
5ch, 100GHz	10Gbit/s NRZ	990	SSMF	~83	PPLN	2003, [27]
7ch, 25GHz	10Gbit/s NRZ	800	SSMF	100	PPLN	2004, [28]
1ch	40Gbit/s RZ-DPSK	6,400	TWRS+DCF	100	PPLN	2004, [4]
16ch, 100GHz	40Gbit/s NRZ	800	SSMF	100	PPLN	2004, [29]
4ch, 100GHz	40Gbit/s CSRZ	4,800	TWRS+DCF	100	PPLN	2004, [7]
20ch, 100GHz, 50GHz, 25GHz	40Gbit/s NRZ + Duobinary + 10Gbit/s NRZ	800	SSMF	100	PPLN	2004, [32]
22ch, 50GHz	20Gbit/s RZ-DQPSK	10,200	SSMF	94.5	PPLN	2005, [39]

using EDFAs for signal amplification [28]. In this experiment, a 3-dB penalty in received power was measured when the channel spacing was reduced from 50 to 25 GHz; hence, the capability for OPC to compensate for XPM is questionable. We conjecture that better XPM compensation can be achieved by employing Raman amplification to create a more power symmetric transmission link. The first multispan WDM experiment at 40 Gb/s is shown in [29], where 16 channels are transmitted over 800 km of SSMF. Future long-haul WDM transmission systems will likely employ alternative modulation formats as well as 40 Gb/s data rates. It is foreseen that many transmission links will be upgraded on a per channel basis, resulting in mixed data rates and mixed modulation formats in the same fiber. As shown in [32], OPC can be employed to transmit different modulation formats and data rates over the same line without the use of a periodic dispersion map.

OPC experiments have also been reported where OPC is added to a "conventional" transmission link. In such a system, the OPC is used to compensate only for the Kerr effect. The transmission limit of a single channel 40-Gb/s DPSK was extended from 5200 to 6400 km due to the compensation of intrachannel nonlinear impairments [4], [5]. As well compensation of intrachannel nonlinear impairments has been shown for WDM CSRZ, extending the maximum transmission to 4800 km [7]. Recently, ultralong-haul transmission of 22 channels of 20-Gb/s DQPSK over 10 200 km has been reported. In this experiment, OPC is employed to compensate for the chromatic dispersion as well as Kerr effect induced nonlinear impairments [39], [40].

IV. WDM TRANSMISSION EMPLOYING OPC FOR CHROMATIC DISPERSION COMPENSATION

In this section, two WDM transmission experiments will be discussed using OPC for chromatic dispersion compensation. Section IV-A covers the transmission of 16×42.7 Gb/s over 800-km SSMF. Section IV-B discusses the experiment, where different modulation formats and data rates (40-Gb/s NRZ, 40-Gb/s duobinary, and 10-Gb/s NRZ) are transmitted over the same transmission link.

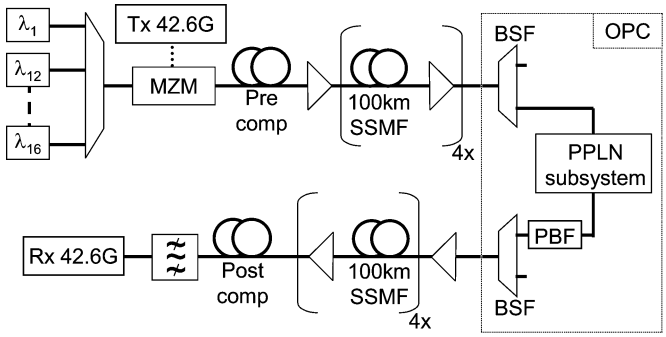

Fig. 6. Experimental setup of the 16×42.7-Gb/s transmission.

A. 16×42.7 Gb/s NRZ Over 800 km

In this experiment, 16×42.7 Gb/s NRZ is transmitted over an 800-km straight line of SSMF [29]. The experimental setup is shown in Fig. 6. Sixteen 100-GHz-spaced CW channels with wavelengths ranging from 1548.5 to 1560.6 nm are multiplexed in an AWG multiplexer and modulated at 42.7 Gb/s with a $2^{31} - 1$ pseudorandom bit sequence (PRBS). After the modulator -510 ps/nm precompensation is applied, optimized to obtain the highest Q-factor after transmission.

After modulation, the data are sent into the transmission link, consisting of eight 100-km spans of SSMF with the span loss varying between 21 and 24 dB. The OPC unit is located midlink, thus after four spans. At the OPC unit, the wavelengths 1548.5, . . ., 1560.6 nm are converted to 1543.7, . . ., 1531.9 nm. Before the data signals are inserted into the PPLN subsystem, a band selection filter (BSF) removes the out of band ASE. After the PPLN subsystem, the pump signal is removed by a passband filter (PBF) and the original data signals are filtered through a BSF. The PPLN subsystem used in this experiment is based on the parallel polarization diversity scheme, as discussed in Section II-B, with a polarization-dependent loss (PDL) of less than 0.5 dB. The two PPLN waveguides used are Magnesium-oxide-doped (MgO:PPLN). Quasi-phase matching inside the PPLN waveguide is realized with a phase matching period of 17.1 μm and a temperature controller at 90 °C. The optical power

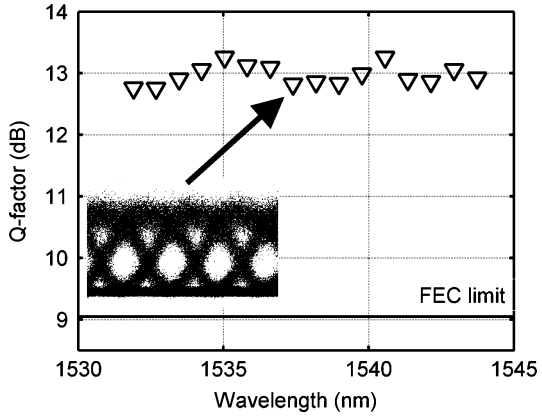

Fig. 7. Q-factors of all 16 WDM channels.

of the pump signal is set to 150 mW per PPLN waveguide. With this configuration, the conversion efficiency is about -16.5 dB. After transmission, the chromatic dispersion is optimized on a per-channel basis using a tunable dispersion compensator. Subsequently, the signal is amplified, filtered with a 0.8 nm tunable bandpass filter, and detected using a bit error rate (BER) test set.

The measured OSNR after transmission is larger than 23.5 dB for all 16 channels. Fig. 7 depicts the Q-factors of all the 16 channels before FEC. Throughout this paper, BER values are measured and converted to Q-factors in dB by

$$Q[\mathrm{db}] = 20\log(Q) = 20\log(\sqrt{2} * \mathrm{erfc}^{-1}(2 * \mathrm{BER})). \quad (4)$$

The Q-factor of the best and the worst channel are 13.3 and 12.8 dB, respectively. These Q-factors are more than 3 dB above the forward error correction (FEC) threshold of the concatenated code RS(255, 247) + RS(247, 239) with a 7% redundancy, for which a Q of 9 dB correspond to error-free transmission after FEC (BER after FEC $< 10^{-12}$) [44]. The inlay of Fig. 7 depicts the eye pattern obtained for channel 8 (1537.4 nm after transmission). The 42.7-Gb/s transmission is OSNR limited, since the Q-factors after transmission are similar to the Q-factor (13.1 dB) measured in a back-to-back configuration at the same OSNR of 23.5 dB.

B. Transparent Chromatic Dispersion Compensation

It is foreseen that in future transmission systems, different modulation formats and data rates are used simultaneously in the same transmission line. The experiment discussed in this section describes the WDM transmission of 42.7-Gb/s NRZ, 42.7-Gb/s duobinary and 10-Gb/s NRZ over the same transmission line [32]. Fig. 8 depicts the experimental setup.

At the transmitter all channels, 42.7-Gb/s NRZ, 10-Gb/s NRZ, and 42.7-Gb/s duobinary, are combined using a star coupler. All signals are copolarized in order to create worst-case interchannel interactions. The PRBS length for all modulation formats is

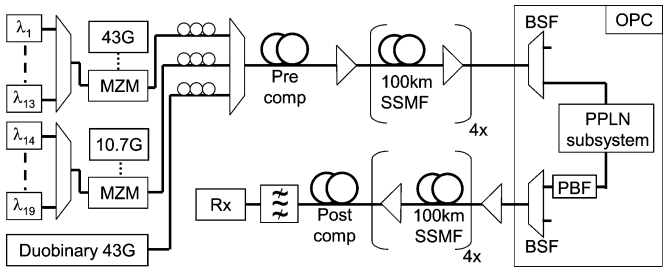

Fig. 8. Experimental setup of WDM 42.7-Gb/s NRZ, 42.7-Gb/s duobinary and 10-Gb/s NRZ transmission.

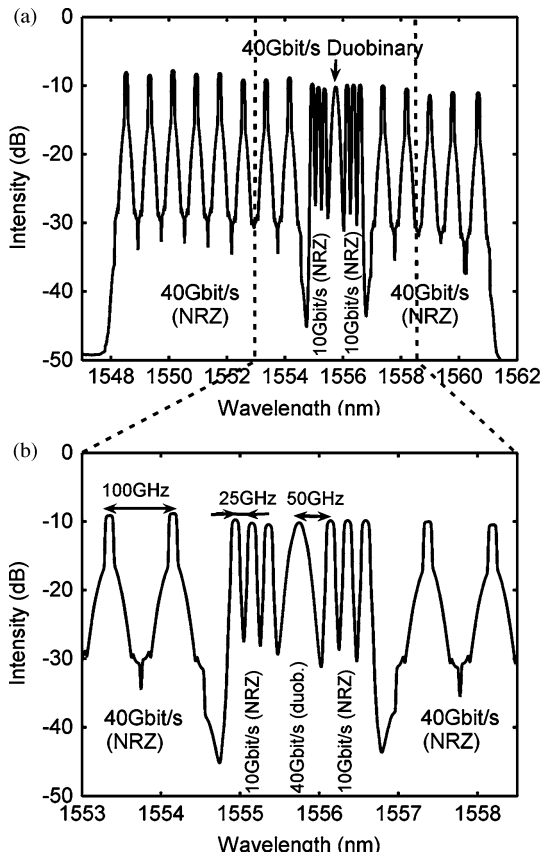

Fig. 9. Optical spectra with a resolution bandwidth of 0.1 nm. (a) Output of the transmitter. (b) Output of the transmitter, zoomed in on the 42.7-Gb/s duobinary and 10-Gb/s NRZ channels.

$2^{31} - 1$. After the transmitter a DCF module with a chromatic dispersion of $D_{\mathrm{dec}} = -170$ ps/nm is used for precompensation.

The transmission link and OPC unit are similar to those described in Section V-A. The SSMF input power is set to 0.8 dBm/channel for all 10-Gb/s channels and to 2.8-dBm/channel for all 42.7-Gb/s channels (NRZ and duobinary). At the end of the transmission link, a tunable dispersion compensator is used to optimize the residual chromatic dispersion at the receiver. Finally, the channels are filtered with a 0.8, 0.4, and 0.2-nm optical bandpass filter for the 42.7-Gb/s NRZ, 42.7-Gb/s duobinary, and 10.7-Gb/s NRZ channels, respectively.

The 20 data channels at the transmitter are shown in Fig. 9(a). A more detailed plot on the positioning of the

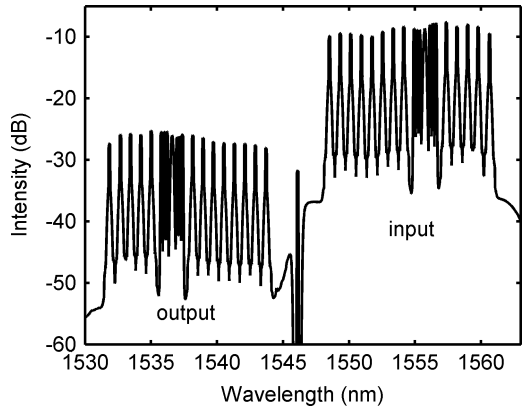

Fig. 10. Optical spectrum after the PBF and the PPLN subsystem (resolution bandwidth 0.1 nm).

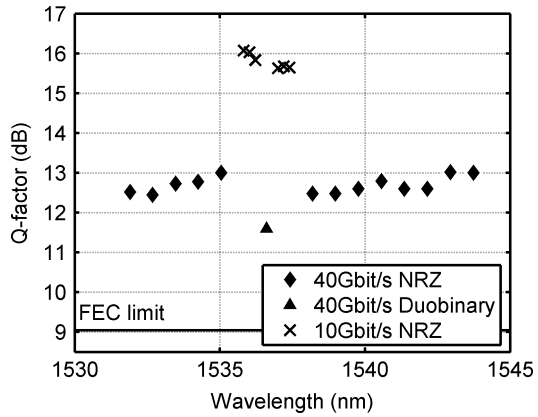

Fig. 11. Q-factor after transmission for all 20 channels.

42.7-Gb/s duobinary channel and the six 10-Gb/s channels can be seen in Fig. 9(b). The 42.7-Gb/s duobinary data channel is launched at 1555.8 nm (before the OPC unit). At 50-GHz spacing, on each side of the duobinary channel, three 25-GHz spaced 10-Gb/s data channels are placed. The 10-Gb/s data channels are surrounded by 13×42.7-Gb/s channels placed on a 100 GHz grid. All channels together cover the higher wavelength part of the C-band ranging from 1548.5 to 1560.6 nm.

Fig. 10 depicts the optical spectrum after passing through the optical phase conjugator, but before the filters used to suppress the input channels. All data channels are converted from the higher part of the C-band to the lower part. In the middle of the plot, at 1546.1 nm, the residual of the suppressed pump can be seen. The OSNR after transmission is greater than 20.5 and 22.3 dB for all 10-Gb/s NRZ and 42.7-Gb/s NRZ channels, respectively. The 42.7-Gb/s duobinary channel had an OSNR of 23.6 dB. Fig. 11 depicts the Q-factors, before FEC of all twenty data channels.

For the 10-Gb/s NRZ channels (plotted as crosses in Fig. 11), Q-factors before FEC are measured varying between 16.1 and 15.4 dB. Due to the narrow channel spacing of 25 GHz, an OSNR penalty of about 1 dB is present from cross-phase modulation. For the 42.7 Gb/s duobinary channel (plotted as a triangle in Fig. 11), a Q-factor is measured of 11.6 dB, which is lower than the Q-factors of all the 42.7-Gb/s NRZ channels, still the Q-factors of the duobinary channel is more than 2 dB above the FEC threshold as defined in [41].

The Q-factors of the 13 42.7 Gb/s NRZ data channels (plotted as diamonds in Fig. 11) varied between 12.3 and 13 dB. These Q-factors are slightly worse than the performance measured in the 16×42.7-Gb/s transmission experiment discussed in Section IV-A, resulting from a slight OSNR degradation due to the more complicated transmitter structure. The 42.7-Gb/s channels are OSNR limited, since the performance after 800 km is similar to the back-to-back performance.

V. Compensation of Nonlinear Distortions

In this section, a description of the compensation of impairments due to intrachannel nonlinear effects (Section V-A) and nonlinear phase noise (Section V-B) is discussed.

A. Intrachannel Nonlinear Effects

At high data-rates, for example 40 Gb/s and more, transmission is mostly in the pseudo linear regime. The psuedo linear regime is defined as the regime where the optimum accumulated dispersion for single channel transmission is almost zero. In this regime, intrachannel nonlinear effects are generally the dominating impairment limiting transmission reach [42]. The compensation of intrachannel nonlinear impairments by OPC has been demonstrated in [26]. In this single channel experiment, 100-Gb/s return-to-zero (RZ) is transmitted over 160 km. Nonlinear effects increase at higher launch power. The impact of nonlinear effects on the Q-factor can be assessed by measuring the Q-factor after transmission as a function of the optical input power into the fiber. Introducing backward Raman pumping in an OPC aided transmission link significantly increases the nonlinear tolerance, due to a more symmetric power envelope. The launch power can be increased by almost 5 dB, since more intrachannel nonlinear impairments are compensated for by OPC. Chowdhury *et al.* showed that in a transmission line, where no power symmetry is present, intrachannel nonlinear impairments can also be compensated for by the means of OPC [4], [5]. In this experiment, the performance of long-haul 40-Gb/s DPSK transmission is compared with and without OPC. The OPC unit is used for the compensation of intrachannel nonlinear impairments only. When the OPC unit is introduced into the transmission link, a two-decade BER improvement is obtained.

The compensation of intrachannel nonlinear impairments is further shown for WDM 40-Gb/s transmission with CSRZ modulation [7]. In this experiment, a 400-km truewave reduced dispersion slope (TWRS) reentrant recirculating loop is employed to assess the transmission performance. The fiber input power and precompensation are optimized for the case with and without OPC. The optimum fiber input power per channel is found to be 1 and -1 dBm for the case with and without the OPC unit, respectively. A hybrid Raman/EDFA structure is used for signal amplification. Midlink, after six circulations, the signals are fed through the PPLN waveguide used for OPC. In this experiment, the pump wavelength is set to 1553.9 nm. The polarization of both the pump and the data signals are copolarized and propagate through the PPLN waveguide in the TM mode.

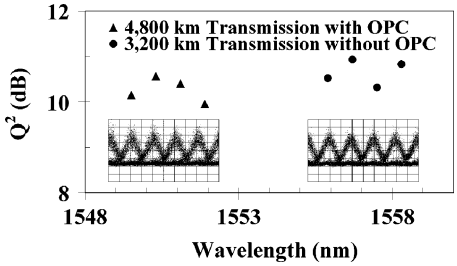

Fig. 12. Performance of WDM channels with (4800 km) and without OPC (3200 km) and corresponding eye diagrams of the worst channels in each case are shown. Q^2 [dB] is defined as $Q^2[\text{dB}] = 10\log(Q^2)$ and is equivalent to Q [dB], which is used throughout the text [7].

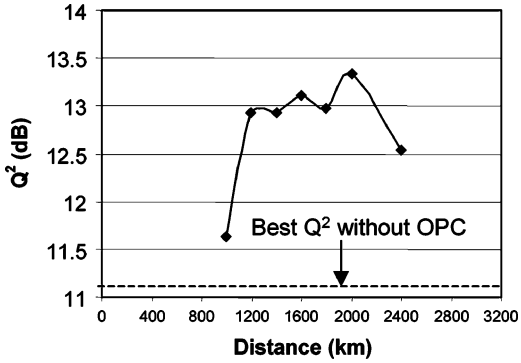

Fig. 13. Transmission performance as a function of the location of the OPC unit. Q^2 [dB] is defined as $Q^2[\text{dB}] = 10\log(Q^2)$ and is equivalent to Q [dB], which is used throughout the text [6].

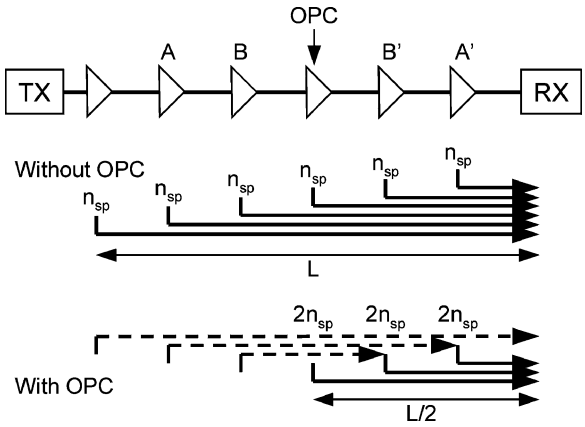

Fig. 14. Mechanism for phase noise compensation as introduced by Lorattanasane and Kikuchi [3].

For the phase-conjugated channels, the sign of the cumulative chromatic dispersion is inverted. In order to restore the inline dispersion map as in the non-OPC configuration, a DCF module is used after the OPC unit to compensate for the change in accumulated chromatic dispersion induced through OPC. For OPC, an annealed proton exchanged PPLN is used, operated at 54.5 °C. A pump power of 110 mW is present at 1553.9 nm and each of the input channels is amplified to 10 mW per channel. The conversion efficiency in this configuration is approximately -15 dB.

Fig. 12 depicts the performance of all four channels after transmission with and without OPC. With OPC the Q-factor varied between 9.9 and 10.5 dB after 4800-km transmission. Without OPC, similar Q values are obtained after 3200-km transmission. Hence, through the compensation of intrachannel nonlinear effects a 50% increase in transmission reach is obtained.

In a similar experiment, Raybon *et al*. assessed the dependence of the Q-factor on the location of the OPC unit along the link by placing the OPC unit in several locations for a constant total transmission distance of 3200 km [6]. In this experiment, only a single channel is modulated with 40-Gb/s CSRZ. In order to enable flexible placement of the OPC unit, the transmission length of the recirculating loop is reduced from 400-to 200-km TWRS fiber and the dispersion map is adjusted such that the accumulated dispersion is near 0 ps/nm. Fig. 13 depicts the transmission performance as a function of the location of the OPC unit. Without OPC, the Q-factor is 11.2 dB. With the OPC unit around the center of the transmission link, the Q-factor increases to $\sim$ 13 dB. The optimum Q value is obtained when the OPC unit is placed at 2000 km. When the OPC unit is placed between 1200 and 2000 km, the Q varies less than 0.5 dB. This corresponds to nearly $1/3$rd and $2/3$rd of the transmission line. It can thus be concluded that for the compensation of intrachannel impairments, the location of the OPC unit is not critical.

B. Nonlinear Phase Noise Compensation

Recently, strong interest has been shown in phase-shift keying (PSK) modulation formats, in order to increase the robustness of the transmission links. However, PSK signals can, unlike on–off keying (OOK) signals, be impaired by nonlinear phase noise. Nonlinear phase noise results from power fluctuations originating from ASE noise that are converted into phase fluctuations of the signal through the Kerr effect, and is commonly referred to as the Gordon–Mollenauer effect [43], [44]. Transmission impairments due to nonlinear phase noise can be compensated for by OPC. Initially the compensation of phase noise through OPC has been proposed by Lorattanasane and Kikuchi for a long-haul on–off keying coherent transmission line [3]. The principle is however, applicable to phase shift keyed transmission as well. In a coherent transmission system, phase sensitive detection occurs at the receiver using a local oscillator. Fluctuations in the phase of the received signal on the bit-level impair system performance because the local oscillator cannot correct for the fast phase changes, hence the impact of this impairment is similar to PSK-based transmission. The mechanism for phase noise compensation by midlink OPC is depicted in Fig. 14. In this example, a system with six spans is discussed with and without OPC.

At the receiver, the accumulated phase noise is proportional to $n_{\text{sp}}L^3$ where n_{sp} denotes the spontaneous emission factor of the EDFA, which provides a measure for the generated amount of ASE and L the total system length. When midlink OPC is employed, the nonlinear phase noise generated by the Kerr effect

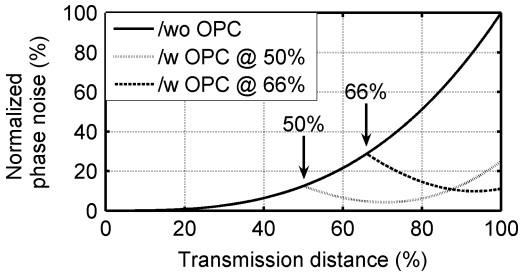

Fig. 15. Normalized phase noise as a function of the transmission distance [45].

can be partly compensated for. In the six span example depicted in Fig. 14, it can be seen that the phase noise introduced by amplifier B is compensated for when the signal reaches amplifier B′. Through the Kerr effect, the power fluctuations originating from ASE noise generated by amplifier B generate phase fluctuations (phase noise) while propagating in the first half of the system. This phase noise is compensated for by OPC in the second half of the system. When the signal reaches amplifier B′ the amount of phase noise caused by the ASE from amplifier B is compensated for. It can be found that the accumulated phase noise variance in this case is proportional to $(2n_{\rm sp})(L/2)^3 = n_{\rm sp}L^3/4$, resulting in about 6-dB phase noise suppression [3]. McKinstrie *et al*. showed in [45] that the 6-dB phase noise reduction through midlink OPC can be achieved as well for differential PSK systems. The phase noise reduction can be increased to 9.5 dB, when the OPC unit is placed at 66% of the transmission line. In that case, however, OPC cannot compensate for the chromatic dispersion of the total transmission link. Fig. 15 depicts the normalized phase noise as a function of the transmission distance for the OPC placed at 50% and 66% along the transmission line.

Note that this is only the case when the phase noise solely originates from ASE of the amplifiers in the transmission line. Another impairment resulting in nonlinear phase noise is imperfections of the modulated signal at the transmitter (e.g., a broad "1" level for DQPSK signals). This can be treated equivalent to an amplifier at the transmitter with a high noise factor, and will, hence, shift the optimal position of the OPC toward the middle of the link. Alternatively, two OPC units can be employed to obtain a further reduction of nonlinear phase noise. In order to obtain full compensation of the chromatic dispersion, the OPC units must be placed at X % and $(X + 50)$% in the transmission line, with X a fraction of the transmission line between 0% and 50%. The optimal phase noise suppression is obtained when the OPC units are placed at 25% and 75% of the transmission line. The accumulated phase noise variance is than proportional to $2(2n_{\rm sp})(L/4)^3 = n_{\rm sp}L^3/16$, resulting in about 12-dB phase noise suppression [3], [45]. The phase noise suppression can be increased to 14 dB by placing the OPC units at 40% and 80% of the transmission line, which, however does not result in full dispersion compensation [45]. Table II gives an overview of the predicted phase noise reduction and amount of dispersion compensation feasible for different configurations with one and two OPC units.

TABLE II
PREDICTED PHASE NOISE REDUCTION AND DISPERSION COMPENSATION FOR DIFFERENT OPC CONFIGURATIONS

	1 OPC 50%	1 OPC 66%	2 OPCs 25/75%	2 OPCs 40/80%
Phase noise reduction (dB)	6	9.5	12	14
Dispersion Comp. (%)	100	66	100	80

Due to the periodic power amplification in a long-haul transmission link modulation instability (MI) sidebands can occur and compensation of nonlinear phase noise by means of OPC can be less effective [46]. MI can be mitigated by managing the local dispersion with a periodic dispersion map. [47] Hence, for transmission systems using DCF for periodic chromatic dispersion compensation MI is not of significance. For transmission systems using OPC for dispersion compensation MI might impair the performance but results reported so far have not shown MI induced degradation [31], [40]. Since for high values of chromatic dispersion (e.g., SSMF) the impact of MI is decreased [3], we conjecture that for the SSMF fiber type the contribution of MI is relatively small.

Section V-B describes a proof-of-principle experiment showing compensation of impairments due to nonlinear phase noise by means of OPC. In order to show nonlinear phase noise impairments, the effect is enhanced by noise loading (artificially reducing the OSNR) at the transmitter (to increase the power fluctuations due to ASE noise) and using high input powers into the SSMF (to enhance SPM). The influence of nonlinear phase noise can be measured, by comparing the performance of the system for different amounts of noise loading at the transmitter, while keeping the OSNR at the receiver constant. When noise loading occurs at the transmitter, strong power fluctuations due to ASE will occur along the transmission line and hence a strong influence of nonlinear phase noise will be present. Note that in this configuration the noise is introduced at the transmitter (amplifier A in Fig. 14) and does not accumulate along the transmission line. Since in a real-world transmission system noise accumulates along the line, the impact of nonlinear phase noise will likely be smaller and compensation schemes less effective.

The experimental setup of the proof-of-principle experiment is depicted in Fig. 16 and in [8], [9]. In this experiment, the Q-factor is measured as a function of the transmitted OSNR. The noise generation scheme at the transmitter and the receiver, which enables setting the OSNR of the data signal, consist of an attenuator, an optical amplifier and a band pass filter. The input powers into the SSMF and DCF are 11.5 and 1.5 dBm, respectively. The compensation of nonlinear phase noise is studied by inserting an OPC unit midlink and evaluating the performance difference.

Fig. 17 shows the performance after 800-km transmission as a function of the transmitted OSNR for DPSK and OOK without the OPC unit. The OSNR after transmission is kept constant at 12 dB by additional noise loading at the receiver. At high transmitted OSNR (40 dB), DPSK performs over 2 dB better in

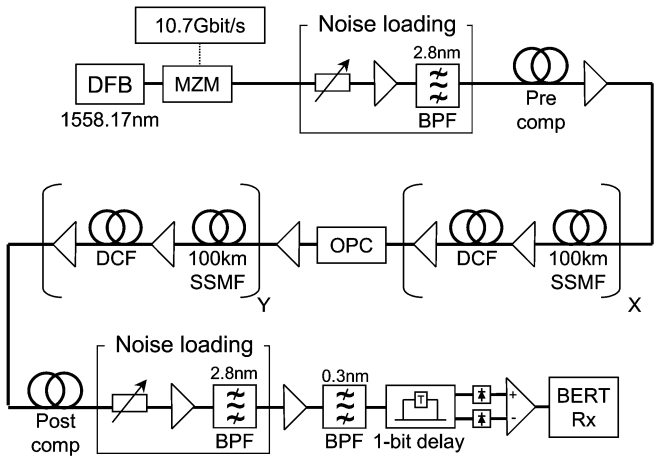

Fig. 16. Proof-of-principle experimental showing the influence of nonlinear phase noise on DPSK transmission.

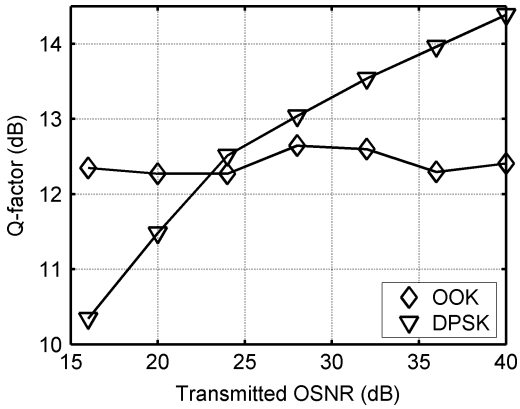

Fig. 17. Q-factor as a function of the transmitted OSNR for the DPSK and OOK modulation format without OPC.

Q-factor than OOK. Similar to the results reported in [44], the Q-factor of DPSK is severely affected by nonlinear phase noise when the OSNR of the transmitter is reduced, whereas for OOK, the Q-factor is unaffected. As a result, when the transmitted OSNR is reduced to 16 dB, the performance of DPSK is worse in comparison to OOK.

In order to study the effect of OPC on nonlinear phase noise, the phase conjugator is inserted in the middle of the link. In this single channel experiment, OPC is realized by FWM in a SOA. A more detailed description of the OPC unit can be found in [8]. The polarization of the pump and the data signals are copolarized before entering the SOA. Midlink OPC can be used to compensate for the chromatic dispersion (as described in Section IV). In such an application, the inline DCF is removed from the transmission line resulting in a nonperiodic dispersion map. In a "conventional" DCF aided transmission link a periodic dispersion map is used, since the chromatic dispersion is compensated for after each span. In this proof-of-principle experiment, the effect of a nonperiodic dispersion map on the nonlinear phase noise penalty is excluded by using the same effective dispersion map with and without OPC. Similar to the experiments described in Section V-A, the change in accumulated

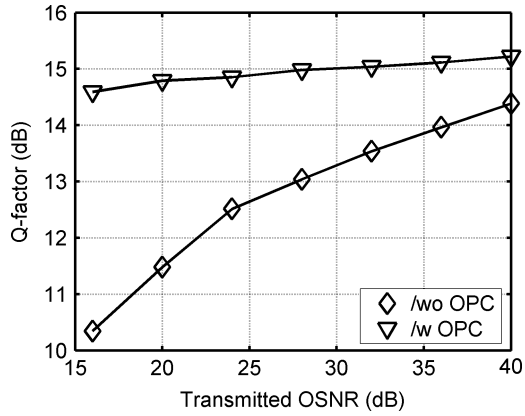

Fig. 18. Q-factor as a function of the transmitted OSNR for DPSK transmission /wo OPC and /w OPC. The "/wo OPC" curve corresponds to the "DPSK" curve, as shown in Fig. 17.

chromatic dispersion induced through OPC is compensated for using a DCF module after the OPC unit.

The Q-factor as a function of the transmitted OSNR for the transmission system with and without OPC is plotted in Fig. 18. At high transmitted OSNR (40 dB), where the effect of the nonlinear phase noise is low, the OPC-based configuration shows about 1-dB improvement in Q-factor compared to the DCF-based configuration. Simulations reported in [9] show that this improvement in Q-factor at high-transmitted OSNR results from a compensation of SPM by OPC. At low-transmitted OSNR (16 dB), the performance of the system without OPC is impaired by over 4 dB in Q-factor due to nonlinear phase noise, whereas the Q-factor of the OPC-based system is degraded by less then 1 dB. We can hence conclude that in this configuration, most of the nonlinear phase noise is compensated for. The 1-dB degradation in Q-factor that is present when the OSNR of the transmitter is reduced originates partly from the nonsymmetric power envelope of the transmission line with respect to the OPC unit. Furthermore, as predicted in Fig. 14, nonlinear phase noise, caused by ASE of the inline amplifiers, is not completely compensated with a single OPC unit.

VI. Ultralong-Haul RZ-DQPSK Transmission

RZ-DQPSK is a promising modulation format for future transmission systems. In this section, an ultralong-haul transmission experiment is described comparing the performance of DCF- and OPC-aided transmission [39], [40].

A. Experimental Setups

The experimental setups of the DCF- and the OPC-based configurations are depicted in Fig. 19. In both experiments, the transmitter and receiver structures are the same. At the transmitter, 44 WDM DQPSK channels are generated on a 50-GHz grid by a modulator cascade consisting of two external $LiNbO_3$ Mach–Zehnder modulators (MZM). The first modulator is driven with a 10.7-GHz clock signal, carving a pulse with a 50% duty cycle. The second modulator is an integrated DQPSK modulator with two parallel MZMs within a super Mach–Zehnder

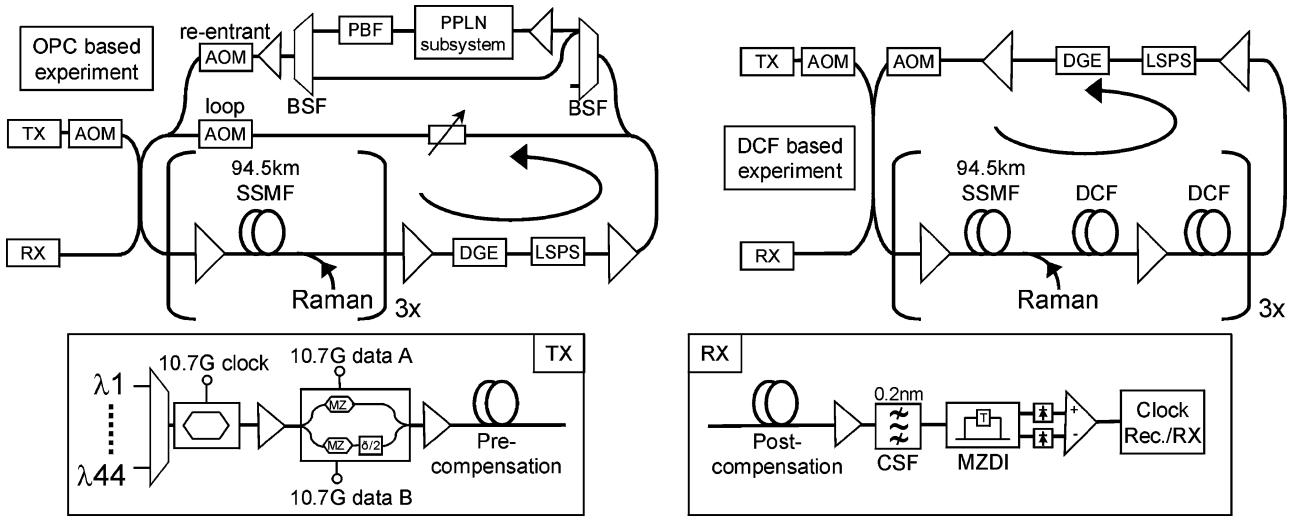

Fig. 19. Experimental setups of the OPC- and DCF-based recirculating loop.

structure. The relative phase shift between the two parallel modulators is $\pi/2$. Two 10.7-Gb/s data streams with a relative delay of 5 b for decorrelation of the bit sequences are used for modulation of the 21.4-Gb/s DQPSK signal (two 10.7-Gb/s data streams, an in-phase and a quadrature component, are thus effectively multiplexed into one 21.4-Gb/s DQPSK channel). The DQPSK modulation format requires the BERT to be programmed for the expected output sequence. In this experiment, a PRBS length of $2^{15}-1$ is used because programming the expected output sequence makes longer sequences impractical. Alternatively, precoding of both data sequences can be used, which does not restrict the length of the PRBS [48].

The reentrant recirculating loop consists of three 94.5-km spans of SSMF with an average span loss of 21.5 dB and a chromatic dispersion of $\sim$16 ps/nm/km. The loss of the SSMF spans is compensated for by using a hybrid Raman/EDFA structure for signal amplification. The average on/off Raman gain of the backward pumped Raman pumps is $\sim$11 dB. A loop-synchronous polarization scrambler (LSPS) is used to reduce the statistical correlation of loop-induced polarization effects. Power equalization of the DWDM channels is provided by a channel-based dynamic gain equalizer (DGE) with a bandwidth of 0.3 nm, hence, spectral filtering of the signals occurs with every re-circulation.

The signals are optically phase conjugated in the middle of the transmission link. In the reentrant recirculating loop structure, this is realized after half the recirculations $(18\times)$ by opening the loop acoustooptic modulator (AOM) and closing the reentrant AOM for one recirculation. Hereby, the signals are fed through the PPLN subsystem. In this subsystem, the 22 channels from 1532.3 to 1540.6 nm, used to balance the signal in the amplifiers, are removed using a BSF. Subsequently, the remaining 22 channels from 1546.1 to 1554.5 nm are phase conjugated in the counter-directional polarization diversity structure. At the output of the polarization diversity structure, the phase-conjugated signals are present mirrored with respect to the pump and range from 1532.3 to 1540.6 nm. The optical spectrum after the polarization diversity structure is depicted in Fig. 20.

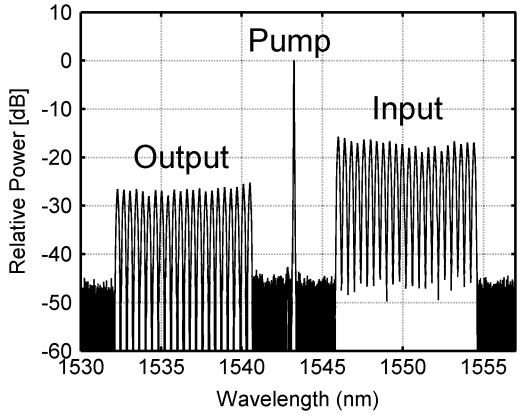

Fig. 20. Optical spectrum at the output of the PPLN subsystem after 18 circulations in the loop (resolution bandwidth = 0.01 nm).

In this spectrum the pump signal, original data signals and phase-conjugated signals can be seen. After the polarization diversity structure, the pump signal is suppressed through a PBF and the original data signal is removed using a band selection filter. Finally, the original channels of the PPLN subsystem (ranging from 1546.1 to 1554.5 nm) are recombined with the spectrally inverted channels to balance the signal propagating through another 18 circulations in the recirculating loop. In this experiment, the OPC unit compensates for an accumulated chromatic dispersion of over 160 000 ps/nm. The input power per channel into the SSMF is -2.9 dBm (13.5 dBm total input power).

The PPLN subsystem used in this experiment is based on the counter propagating polarization diversity scheme as discussed in Section II-B. The measured PDL of the PPLN subsystem is less than 0.4 dB. A continuous wave (CW) pump signal is generated at 1543.4 nm, using an external cavity laser (ECL) and amplified to 388 mW. The power of the signal is approximately 10 mW per channel at the PBS. The conversion efficiency of the PPLN waveguide with these powers is -9.2 dB. The PPLN waveguide used for OPC operates at 202.3 °C, in order to

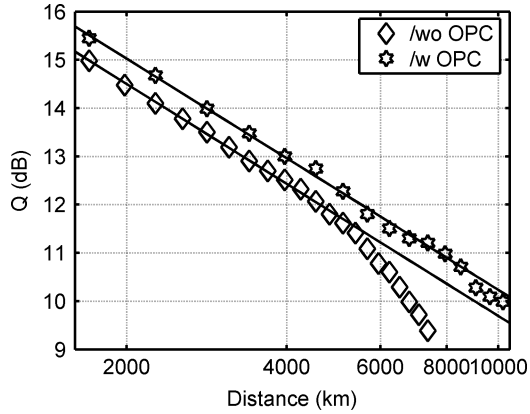

Fig. 21. Q-factor of a typical channel as a function of transmission distance, /wo OPC and /w OPC.

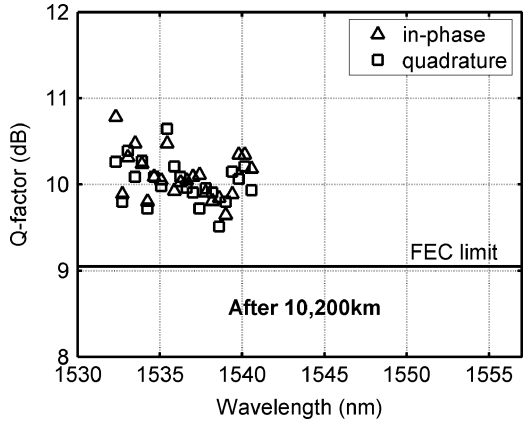

Fig. 22. In-phase and quadrature Q-factors for the midlink OPC-based configuration.

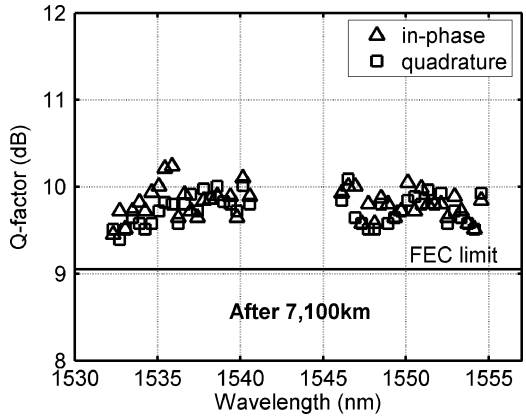

Fig. 23. In-phase and quadrature Q-factors for the DCF-based configuration.

reduce the photorefractive effect. Quasi phase matching inside the PPLN waveguide is realized by reversing the sign of the nonlinear susceptibility every 8.15 μm.

In the DCF-based configuration, the PPLN-subsystem is removed and DCF modules are inserted after each span for chromatic dispersion compensation. 20% of the DCF is placed between the Raman pump and the first stage of the inline amplifier to balance the DCF insertion loss. In order to optimize the performance of the DCF-based transmission system, the optical input power into the SSMF, precompensation and inline dispersion map are optimized at 4500-km transmission distance. The optimization of the transmission performance if further discussed in [49]. The precompensation used is -850 ps/nm and the optimal input power is determined to be -4 dBm/channel, which is 1-dB lower than the input power used in the OPC-based transmission experiment (-3 dBm). The inline dispersion map is found to be optimal at high undercompensation per span, thus an under compensation of around 80 ps/nm/span is used. After transmission, the dispersion is optimized on a per channel basis. A 0.2 nm channel-selection filter (CSF) is used to select the desired channel. After a 1-b (94 ps) Mach–Zehnder delay interferometer (MZDI) and a balanced detector, the clock is recovered and the performance of the signal is evaluated using a BERT.

B. Experimental Results

The Q-factor as a function of the transmission distance is plotted for the OPC and the DCF-based configuration in Fig. 21. The typical channels used in this plot are for the OPC configuration the in-phase at 1535.1 nm and for the DCF configuration the in-phase at 1550.7 nm. At shorter distances, the Q-factor of the DCF-based configuration is about 0.5 dB lower than that of the OPC-based transmission system. After 5000 km transmission, the Q-factor of the DCF-based configuration deviates from the linear decrease, whereas the OPC-based performance is virtually unaffected despite the higher launch power into the SSMF. For the RZ-DQPSK modulation format, it has been shown that single channel impairments are dominant over multi channel impairments [50]. We conjecture that the Q degradation of the DCF-aided transmission results from SPM induced nonlinear impairments, such as nonlinear phase noise. As well, an extra penalty arises in this experiment due to imperfections of the parallel DQPSK modulator (e.g., a broad "1" rail for the DQPSK signal), resulting in additional nonlinear phase noise impairments after transmission. In the OPC aided transmission experiment, the SPM induced nonlinear impairments resulting from both modulator imperfections and transmission line are reduced through midlink OPC, resulting in an increased transmission reach.

Fig. 23 shows the Q-factors for the DCF-based transmission after 7100 km (25 circulations through the recirculating loop). For the OPC-based configuration the same Q values are obtained after 10 200 km (36 circulations), which is a distance increase of 44%. The Q-factors for the OPC aided transmission are plotted in Fig. 22. In Figs. 22 and 23, both the in-phase and quadrature channels are depicted and similar performance is seen for these channels. Note that in the OPC-based configuration, the Q-factor is only evaluated for the 22 phase-conjugated channels. A second OPC unit is required to conjugate the other 22 channels.

In the OPC-based configuration, a wavelength conversion occurs in the middle of the transmission link. Across the C-band, the noise figure of the EDFA/Raman amplifiers can vary resulting in a spectral dependent performance of the WDM

channels [31], which would result in a performance difference between the OPC and the DCF-based configuration. In order to exclude this wavelength dependent noise figure and thereby wavelength dependent performance, the Q-factor of all 44 channels is assessed in the DCF-based configuration. However, in Fig. 23, it can be seen that the Q performance is similar for all channels, and no spectral dependence is measured. The worst Q-factor is 9.5 dB after 10 200-km transmission and 9.4 dB after 7100-km transmission for the OPC and the DCF-based configuration, respectively. These Q-factors are well above the FEC limit as defined in [41].

From this long-haul DQPSK transmission experiment, we conclude that the chromatic dispersion is compensated and nonlinear impairments reduced by using a single PPLN waveguide for OPC.

VII. Outlook

The polarization independent PPLN structure used for OPC discussed in Section VI of this paper offers first-rate conversion efficiency (~ -10 dB) and a single unit is capable of converting a high WDM channel count without a noticeable conversion penalty. In this configuration, at least two extra amplifiers are required (one amplifier to boost the pump signal and one at the input of the OPC-subsystem to amplify the data channels) making OPC a less cost-effective solution. This might offset the performance and cost reduction gains provided through OPC. One could potentially omit the pump booster by reducing the pump power, but this significantly reduces the conversion efficiency. Alternatively, the amplifier for the data channels can be saved by reducing coupling losses, improving the conversion efficiency and increasing parametric amplification of the PPLN waveguide [51].

Due to the wavelength conversion in the OPC subsystem a second PPLN waveguide would be required to phase conjugate all channels of a full band WDM system. Alternatively, as demonstrated by Kurz *et al*. [52], mode multiplexing in a PPLN waveguide can be employed for bidirectional phase conjugation. In such an OPC subsystem, higher order waveguide modes are used to separate the input signal from the phase-conjugated signal, using asymmetric Y junctions. Mode multiplexing would simplify the design of the OPC subsystem, omitting filters to remove the input channels and minimizing the wavelength shift inherent to OPC.

Apart from the PPLN waveguide, other media such as AlGaAs are suitable to create OPC through DFG. Multi channel OPC using an AlGaAs waveguide has been shown by Yoo *et al*. [53]. A great advantage of AlGaAs is that it can be designed to be polarization insensitive [54] and does not suffer from restrictions due to the photorefractive effect. Furthermore, AlGaAs has a higher nonlinear coefficient than lithium niobate. Although, the conversion efficiency shown so far is relatively low, this technique could potentially yield a high conversion OPC unit.

Ideally, these developments will yield an OPC subsystem that is transparent with respect to insertion loss, which would greatly ease the application of OPC in real-world applications.

Considering the advantages of OPC for transmission applications, we mainly see potential in high data rate transmission. Transmission systems operating at a 10-Gb/s line rate have been greatly optimized in recent years and further development foremost focuses on providing low-cost but robust solutions. For 40-Gb/s transmission, we believe that especially DQPSK modulation format offers significant advantages in providing a robust solution for high-capacity long-haul transport. DQPSK has a favorable spectral width making it robust against narrow band filtering. Furthermore, it has a higher PMD and chromatic dispersion tolerance at the same effective data rate as binary modulation, possibly easing deployment of 40-Gb/s transmission over legacy fiber. A concern, however with DQPSK is possible impairments by SPM induced nonlinear impairments, such as nonlinear phase noise. Based on the obtained results for 20-Gb/s DQPSK, we expect that the transmission performance of 40-Gb/s DQPSK, using OPC provides an excellent robustness against SPM induced nonlinear impairments and hence could be a robust solution for future long-haul transport systems.

VIII. Summary and Conclusion

In this paper, several recent transmission experiments and aspects of OPC have been discussed. The discussion focused on both compensation through midlink OPC of nonlinear penalties and the compensation of chromatic dispersion. For OPC, DFG in a PPLN waveguide is used in most experiments. The PPLN waveguide offers high conversion efficiency (~ -10 dB), is capable of WDM conversion and does not distort the signal during the conversion process. To overcome the polarization dependence a polarization diversity structure is employed. Both a parallel and a counter-directional polarization diversity structure are described, to avoid the polarization dependence of the PPLN waveguide.

Using OPC, the compensation of chromatic dispersion for 40-Gb/s WDM transmission is presented. In this experiment, 16 40-Gb/s channels are transmitted over 800 km of SSMF with EDFA only amplification. Furthermore, we discussed transparent transmission of 40-Gb/s NRZ, 40-Gb/s duobinary and 10-Gb/s NRZ over 800 km of SSMF. Transparent transmission lines are particularly appealing for network operators, since existing networks can be upgraded without having to replace the equipment, or make changes in the transmission line. Note, however that because of the wavelength conversion in the OPC unit, wavelength mapping would be required on a higher network level.

OPC can be employed to significantly reduce intrachannel nonlinear impairments as well as impairments due to nonlinear phase noise. The compensation of intrachannel nonlinear impairments is discussed in a 4×40-Gb/s WDM ultralong-haul transmission link. By adding an OPC to a transmission line with DCF for dispersion compensation, 50% increase in transmission reach is obtained due to intrachannel nonlinearity compensation. As well, the compensation of impairments due to nonlinear phase noise is reviewed. In a proof-of-principle experiment over 4 dB in Q-factor improvement is reported due to the compensation of nonlinear phase noise impairments.

Finally, transmission of 22×20-Gb/s DQPSK WDM is presented. In this experiment, OPC is used to compensate for chromatic dispersion as well as nonlinear impairments and successful transmission over 10 200 km is demonstrated. For OPC, one polarization independent PPLN subsystem is used to compensate for an accumulated chromatic dispersion of over 160 000 ps/nm. When the performance of OPC aided transmission is compared to "conventional," optimized DCF aided transmission a 44% increase in transmission distance is observed in the case of OPC aided transmission. This performance improvement results from compensation for SPM induced nonlinear impairments, such as nonlinear phase noise.

In summary, we conclude that OPC can be a key technology to increase system robustness and realize future transport systems with high data rates and alternative modulation formats.

ACKNOWLEDGMENT

The authors would like to thank Dr. A. Chowdhury and Dr. G. Raybon from Bell Laboratories for providing Figs. 12 and 13, and Dr. T. Ohara from the NTT Corporation for providing Fig. 2. The authors would also like to thank Dr. M. Sher, Dr. H. Escobar, Dr. S. Field and coworkers from Lightbit for the cooperation with the parallel polarization diversity OPC unit, and Dr. H. Suche and Prof. Dr. W. Sohler from the Universität Paderborn for the cooperation with the counter propagating polarization diversity OPC unit. Furthermore, they would like to thank C. Climent for his work on the reentrant recirculating loop. Finally, the authors would like to thank M. Bohn, A. Schöpflin and C.-J. Weiske from the Siemens AG for their support.

REFERENCES

[1] A. Yariv, D. Fekete, and D. M. Pepper, "Compensation for channel dispersion by nonlinear optical phase conjugation," *Opt. Lett.*, vol. 4, pp. 52–54, 1979.

[2] S. Watanabe and M. Shirasaki, "Exact compensation for both chromatic dispersion and kerr effect in a transmission fiber using optical phase conjugation," *J. Lightw. Technol.*, vol. 14, no. 3, pp. 243–248, Mar. 1996.

[3] C. Lorattanasane and K. Kikuchi, "Design theory of long-distance optical transmission systems using midway optical phase conjugation," *J. Lightw. Technol.*, vol. 15, no. 6, pp. 948–955, Jun. 1997.

[4] A. Chowdhury, G. Raybon, R.-J. Essiambre, J. Sinsky, A. Adamiecki, J. Leuthold, C. R. Doerr, and S. Chandrasekhar, "Compensation of intrachannel nonlinearities in 40-Gb/s pseudo linear systems using optical phase conjugation," presented at the Optical Fiber Communications Conf. (OFC'04), 2004, Post-Deadline Paper PDP 32.

[5] ——, "Compensation of intrachannel nonlinearities in 40-Gb/s pseudolinear systems using optical-phase conjugation," *J. Lightw. Technol.*, vol. 23, no. 1, pp. 172–177, Jan. 2005.

[6] G. Raybon, A. Chowdhury, R.-J. Essiambre, and C. R. Doerr, "Location optimization of a single optical phase conjugator in a 3200-km, 40-Gb/s pseudo-linear transmission system," presented at the Eur. Conf. Optical Communications (ECOC'04), Anaheim, CA, 2004, Paper Th2.5.5.

[7] A. Chowdhury, G. Raybon, R.-J. Essiambre, and C. R. Doerr, "Optical phase conjugation in a WDM CSRZ pseudo-linear 40-Gb/s system for 4800-km transmission," presented at the Eur. Conf. Optical Communications (ECOC'04), Stockholm, Sweden, 2004, Post-Deadline Paper Th4.5.6.

[8] S. L. Jansen, D. van den Borne, C. C. Monsalve, S. Spälter, P. M. Krummrich, G. D. Khoe, and H. de Waardt, "Reduction of Gordon-Mollenauer phase noise by midlink spectral inversion," *IEEE Photon. Technol. Lett.*, vol. 17, no. 4, pp. 923–925, Apr. 2005.

[9] S. L. Jansen, S. Calabró, B. Spinnler, D. van den Borne, P. M. Krummrich, G. D. Khoe, and H. de Waardt, "Nonlinear phase noise reduction in DPSK transmission by optical phase conjugation," presented at the OECC'05, Stockholm, Sweden, 2005, Paper 6B1-3.

[10] R. M. Jopson, A. H. Gnauck, and R. M. Derosier, "Compensation of fibre chromatic dispersion by spectral inversion," *Electron. Lett.*, vol. 29, no. 7, pp. 576–578, Apr. 1, 1993.

[11] A. H. Gnauck, R. M. Jopson, and R. M. Derosier, "l0-Gb/s 360-km transmission over dispersive fiber using midsystem spectral inversion," *IEEE Photon. Technol. Lett.*, vol. 5, no. 6, pp. 663–666, Jun. 1993.

[12] S. Watanabe, S. Kaneko, G. Ishikawa, A. Sugata, H. Ooi, and T. Chikama, "20-Gb/s fiber transmission experiment over 3000-km waveform precompensation using fiber compensator and optical phase conjugator," presented at the IOOC, Hong Kong, 1995, Paper PD2-6.

[13] D. D. Marcenac, D. Nesset, A. E. Kelly, M. Brierley, A. D. Ellis, D. G. Moodie, and C. W. Ford, "40-Gb/s transmission over 406 km of NDSF using midspan spectral inversion by four-wave-mixing in a 2-mm long semiconductor optical amplifier," *Electron. Lett.*, vol. 33, no. 10, pp. 879–880, May 8, 1997.

[14] U. Feiste, R. Ludwig, E. Dietrich, S. Diez, H. J. Ehrke, Dz. Razic, and H. G. Weber, "40-Gb/s transmission over 434-km standard-fiber using polarisation independent midspan spectral inversion," *Electron. Lett.*, vol. 34, no. 21, pp. 2044–2045, Oct. 15, 1998.

[15] S. Watanabe, S. Takeda, G. Ishikawa, H. Ooi, J. G. Nielsen, and C. Sonne, "Simultaneous wavelength conversion and optical phase conjugation of 200 Gb/s (5×40 Gb/s) WDM signal using a highly nonlinear fiber four-wave mixer," in *Proc. ECOC'97*, 1997, pp. 1–4.

[16] S. Watanabe, S. Takeda, and T. Chikama, "Interband wavelength conversion of 320 Gb/s (32×10 Gb/s) WDM signal using a polarization-insensitive fiber four-wave mixer," in *Proc. ECOC'98*, 1998, pp. 85–87.

[17] S. Y. Set, R. Girardi, B. E. Riccardi, B. E. Olsson, M. Puleo, M. Ibsen, R. I. Laming, P. A. Andrekson, F. Cisternino, and H. Geiger, "40-Gb/s field transmission over standard fibre using midspan spectral inversion for dispersion compensation," *Electron. Lett.*, vol. 35, no. 7, pp. 581–582, Apr. 1999.

[18] U. Feiste, R. Ludwig, C. Schmidt, E. Dietrich, S. Diez, H. J. Ehrke, E. Patzak, H. G. Weber, and T. Merker, "80-Gb/s transmission over 160-km standard-fiber using optical phase conjugation in a Sagnac-interferometer," *IEEE Photon. Technol. Lett.*, vol. 11, no. 8, pp. 1063–1065, Aug. 1999.

[19] J. Inoue, H. Sotobayashi, W. Chujo, and H. Kawaguchi, "80-Gb/s OTDM signal transmission over 208-km standard fibre using midspan optical phase conjugation based on four-wave mixing in semidonductor optical amplifiers," *Electron. Lett.*, vol. 38, no. 15, pp. 819–821, Jul. 2002.

[20] S. Radic, R. M. Jopson, C. J. McKinstrie, A. H. Gnauck, S. Chandrasekhar, and J. C. Centanni, "Wavelength division multiplexed transmission over standard single mode fiber using polarization insensitive signal conjugation in highly nonlinear optical fiber," presented at the Optical Fiber Communications Conf. (OFC'03), Atlanta, GA, 2003, Paper PD12.

[21] C. Q. Xu, H. Okayama, and M. Kawahara, "1.5-mm band efficient broadband wavelength conversion by difference frequence generation in a periodically domain-inverted $LiNbO_3$ channel waveguide," *Appl. Phys. Lett.*, vol. 62, pp. 3559–3561, 1993.

[22] M. H. Chou, J. Hauden, M. A. Arbore, and M. M. Fejer, "1.5-mm-band wavelength conversion based on difference-frequency generation in $LiNbO_3$ waveguides with integrated coupling structures," *Opt. Lett.*, vol. 23, pp. 1004–1006, 1998.

[23] Y. Furukawa, K. Kitamura, S. Takekawa, K. Niwa, and H. Hatano, "Stoichiometric $MgLiNbO_3$ as an effectivematerial for nonlinear optics," *Opt. Lett.*, vol. 23, pp. 1892–1894, 1998.

[24] C. Q. Xu, H. Okayama, and Y. Ogawa, "Photorefractive damage of $LiNbO_3$ quasiphase matched wavelength converters," *J. Appl. Phys.*, vol. 87, no. 7, pp. 3203–3208, 2000.

[25] I. Brener, M. H. Chou, G. Lenz, R. Scotti, E. E. Chaban, J. Shmulovich, D. Philen, S. Kosinski, K. R. Parameswaran, and M. M. Fejer, "High efficiency (-7 dB), wideband (70 nm) and tunable $LiNbO_3$-waveguide midspan spectral inverter and its use for dispersion compensation in 4×10 Gbit/s," in *Proc. ECOC'99*, 1999, vol. II, pp. 16–17.

[26] I. Brener, B. Mikkelsen, K. Rottwitt, W. Burkett, G. Raybon, J. B. Stark, K. Parameswaren, M. H. Chou, M. M. Fejer, E. E. Chaban, R. Harel, D. L. Philen, and S. Kosinski, "Cancellation of all Kerr nonlinearities in long fiber spans using a $LiNbO_3$ phase conjugator and Raman amplification," presented at the Optical Fiber Communications Conf. (OFC 2000), Baltimore, MD, 2000, Post-Deadline Paper PD33.

[27] R. Huang, D. Woll, I. White, H. Escobar, L. Marshall, G. Kra, and M. Sher, "Broadband dispersion compensation using midlink spectral inversion enables performance improvement and cost reduction in optical networks," presented at the Nat. Fiber Optic Engineers Conf. Session, Orlando, FL, 2003, Paper D9.

[28] S. L. Jansen, S. Spälter, G.-D. Khoe, H. de Waardt, H. E. Escobar, M. Sher, D. Woll, and D. Zhou, "10-Gb/s, 25-GHz spaced transmission over 800 km without using dispersion compensation modules," presented at the Optical Fiber Communications Conf. (OFC'04), Los Angeles, CA, Feb. 2006, Paper ThT1.

[29] S. L. Jansen, S. Spälter, G.-D. Khoe, H. de Waardt, H. E. Escobar, L. Marshall, and M. Sher, "16×40 Gb/s over 800 km of SSMF using midlink spectral inversion," *IEEE Photon. Technol. Lett.*, vol. 16, no. 7, pp. 1763–1765, Jul. 2004.

[30] S. L. Jansen, G.-D. Khoe, H. de Waardt, S. Spälter, D. Zhou, Q. Shu, and D. Woll, "The impact of asymmetric placement of a spectral inverter in a 40-Gb/s system," presented at the Eur. Conf. Optical Communications (ECOC'04), Stockholm, Sweden, 2004, Paper Th2.5.6.

[31] S. L. Jansen, S. Spälter, G. D. Khoe, H. de Waardt, M. H. Sher, D. Zhou, and S. Field, "Experimental comparison of midlink spectral inversion and 'conventional' DCF-based transmission in a DWDM system at 40 Gb/s," in *Proc. APOC*, 2004, pp. 5625–5639.

[32] S. L. Jansen, G.-D. Khoe, H. de Waardt, S. Spälter, C.-J. Weiske, A. Schöpflin, S. J. Field, H. E. Escobar, and M. H. Sher, "Mixed data rate and format transmission (40 Gb/s NRZ, 40 Gb/s duobinary, 10 Gb/s NRZ) using midlink spectral inversion," *Opt. Lett.*, vol. 29, pp. 2348–2350, 2004.

[33] G. Schreiber, H. Suche, Y. L. Lee, W. Grundkötter, V. Quiring, R. Ricken, and W. Sohler, "Efficient cascaded difference frequency conversion in periodically poled Ti:$LiNbO_3$ waveguides using pulsed and cw pumping," *Appl. Phys. B*, vol. 73, pp. 501–504, 2001.

[34] J. Yamawaku, H. Takara, T. Ohara, K. Sato, A. Takada, T. Morioka, O. Tadanaga, H. Miyazawa, and M. Asobe, "Simultaneous 25-GHz-spaced DWDM wavelength conversion of 1.03 Tbit/s (103×10 Gb/s) signals in PPLN waveguide," *Electron. Lett.*, vol. 39, no. 15, pp. 1144–1145, Jul. 2003.

[35] I. Brener, M. H. Chou, E. Chaban, K. R. Parameswaran, M. M. Fejer, and S. Kosinski, "Polarization-insensitive parametric wavelength converter-based on cascaded nonlinearities in $LiNbO_3$ waveguides," presented at the Optical Fiber Communications Conf. (OFC 2000), Baltimore, MD, 2000, Paper TuF1-1.

[36] D. Caccioli, A. Paoletti, A. Schiffini, A. Galtarossa, P. Griggio, G. Lorenzetto, P. Minzioni, S. Cascelli, M. Guglielmucci, L. Lattanzi, F. Matera, G. M. T. Beleffi, V. Quiring, W. Sohler, H. Suche, S. Vehovc, and M. Vidmar, "Field demonstration of in-line all-optical wavelength conversion in a WDM dispersion managed 40-Gb/s link," *J. Sel. Topics Quantum Electron.*, vol. 10, no. 2, pp. 356–362, Mar./Apr. 2004.

[37] G. P. Agrawal, *Nonlinear Fiber Optics*, 3rd ed. New York: Academic, 2001.

[38] X. Shu, K. Chisholm, and K. Sugden, "Design and realization of dispersion slope compensators using distributed Gires-Tournois etalons," *IEEE Photon. Technol. Lett.*, vol. 16, no. 4, pp. 1092–1094, Apr. 2004.

[39] S. L. Jansen, D. van den Borne, C. Climent, M. Serbay, C.-J. Weiske, H. Suche, P. M. Krummrich, S. Spälter, S. Calabró, N. Hecker-Denschlag, P. Leisching, W. Rosenkranz, W. Sohler, G. D. Khoe, T. Koonen, and H. de Waardt, "10 200 km $22 \times 2 \times 10$ Gb/s RZ-DQPSK dense WDM transmission without inline dispersion compensation through optical phase conjugation," presented at the Optical Fiber Communications Conf. (OFC'05), Anaheim, CA, 2005, Post-deadline Paper PDP28.

[40] S. L. Jansen, D. van den Borne, P. M. Krummrich, G.-D. Khoe, and H. de Waardt, "Experimental comparison of optical phase conjugation and DCF aided DWDM 2×10.7 Gb/s DQPSK transmission," presented at the Eur. Conf. Optical Communications (ECOC'05), Glasgow, U.K., 2005, Paper Th2.2.3.

[41] C. Rasmussen, S. Dey, F. Liu, J. Bennike, B. Mikkelsen, P. Mamyshev, M. Kimmitt, K. Springer, D. Gapontsev, and V. Ivshin, "Transmission of 40×42.7 Gb/s over 5200 km ultrawave fiber with terrestrial 100 km spans using turn-key ETDM transmitter and receiver," presented at the Eur. Conf. Optical Communications (ECOC'02), Copenhagen, Denmark, 2002, Paper PD4.4.

[42] V. Mamyshev and N. A. Mamysheva, "Pulse-overlapped dispersion-managed data transmission and intrachannel four-wave mixing," *Opt. Lett.*, vol. 24, no. 21, pp. 1454–1456, 1999.

[43] J. P. Gordon and L. F. Mollenauer, "Phase noise in photonic communications systems using linear amplifiers," *Opt. Lett.*, vol. 15, no. 23, pp. 1351–1353, 1990.

[44] H. Kim and A. H. Gnauck, "Experimental investigation of the performance limitation of DPSK systems due to nonlinear phase noise," *IEEE Photon. Technol. Lett.*, vol. 15, no. 2, pp. 320–322, Feb. 2003.

[45] C. J. McKinstrie, S. Radic, and C. Xie, "Reduction of soliton phase jitter by in-line phase conjugation," *Opt. Lett.*, vol. 28, pp. 1519–1521, 2004.

[46] X. Tang and Z. Wu, "Nonlinear noise amplification in optical transmission systems with optical phase conjugation," *J. Lightw. Technol.*, vol. 23, no. 5, pp. 1866–1873, May 2005.

[47] ——, "Suppressing modulation instability in midway optical phase conjugation systems by using dispersion compensation," *IEEE Photon. Technol. Lett.*, vol. 17, no. 4, pp. 926–928, Apr. 2005.

[48] M. Serbay, C. Wree, A. Schöpflin, C.-J. Weiske, D. van den Borne, S. L. Jansen, G.-D. Khoe, P. M. Krummrich, P. Leisching, and W. Rosenkranz, "Coding gain of FEC encoded 21.42 Gb/s RZ-D(Q)PSK using an electrical differential quaternary precoder," presented at the Eur. Conf. Optical Communications (ECOC'05), Glasgow, U.K., 2005, Paper We4.P.10.

[49] S. L. Jansen, D. van den Borne, P. M. Krummrich, G. D. Khoe, and H. de Waardt, "Nonlinear phase noise degradation in ultra-long haul 2×10 Gbit/s DQPSK transmission," presented at the OECC'05, Seoul, Korea, 2005, Paper PDP 04.

[50] C. Wree, J. Leibrich, and W. Rosenkranz, "RZ-DQPSK format with high spectral efficiency and high robustness toward fiber nonlinearities," presented at the Eur. Conf. Optical Communications (ECOC'02), Copenhagen, Denmark, 2002, Paper 9.6.6.

[51] W. Sohler, W. Grundkötter, J. H. Lee, Y. H. Min, V. Quiring, H. Suche, R. Schiek, T. Pertsch, F. Lederer, R. Iwanow, and G. I. Stegeman, "All-optical signal processing in periodically poled $LiNbO_3$ waveguide structures," presented at the Eur. Conf. Optical Communications (ECOC'04), Stockholm, Sweden, 2004, Paper Tu 3.4.1.

[52] J. R. Kurz, J. Huang, X. Xie, T. Saida, and M. M. Fejer, "Mode multiplexing in optical frequency mixers," *Opt. Lett.*, vol. 29, no. 6, pp. 551–553, 2004.

[53] S. J. B. Yoo, "Wavelength conversion technologies for WDM network applications," *J. Lightw. Technol.*, vol. 14, no. 6, pp. 955–966, Jun. 1996.

[54] S. J. B. Yoo, C. Caneau, R. Bhat, M. A. Koza, A. Raijhel, and N. Antoniades, "Wavelength conversion by difference frequency generation in AlGaAs waveguides with periodic domain inversion achieved by wafer bonding," *Appl. Phys. Lett.*, vol. 68, no. 19, pp. 2609–2611.

S. L. Jansen (S'02) was born in Maartensdijk, The Netherlands, in 1978. He received the M.Sc. degree in electrical engineering from Eindhoven University of Technology, Eindhoven, The Netherlands, in 2001. Currently, he is working toward the Ph.D. degree in electrical engineering at Eindhoven University of Technology in collaboration with Siemens AG, Munich, Germany.

He has worked as a part of the high-speed research team for the European-funded IST project FASHION on ultrafast optical switching in semiconductor optical amplifiers at Siemens AG. He is the author or coauthor of more than 25 refereed papers and conference contributions. His main research interests include optical regeneration, optical phase conjugation, and alternative modulation formats.

Mr. Jansen was recently awarded the IEEE Lasers and Electro-Optics Society (LEOS) Graduate Student Fellowship (2005).

D. van den Borne (S'04) was born in Bladel, The Netherlands, on October 7, 1979. He received the M.Sc. degree (*cum laude*) in electrical engineering from Eindhoven University of Technology, Eindhoven, The Netherlands, in 2004. Currently, he is working toward the Ph.D. degree in electrical engineering at Eindhoven University of Technology, in collaboration with Siemens AG, on advanced modulation formats for optical communication links.

He was previously with Fuijtsu Laboratories Ltd., Kawasaki, Japan, working on supercontinuum generation and pulse compression.

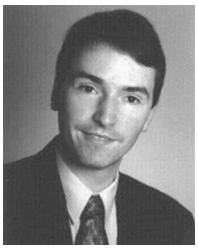

P. M. Krummrich (M'05) received the Dipl.Ing. and Dr.Ing. degrees in electrical engineering from the Technical University of Braunschweig, Braunschweig, Germany, in 1992 and 1995, respectively.

In 1995, he joined Siemens AG, Munich, Germany, where his research focused on distributed erbium-doped fiber amplifiers. Currently, he is working on technologies for the next generation of ultrahigh-capacity DWDM transmission systems with a focus on technologies to enhance system reach such as Raman amplification, advanced modulation formats, adaptive equalizers, and PMD compensation.

S. Spälter was born in Nuernberg, Germany, in 1967. He received the diploma degree in physics from the University of Constance, Konstanz, Germany, in 1994, and the Ph.D. degree from the University of Erlangen, Erlangen, Germany, in 1998, in the field of quantum optics in optical fibers.

From 1998 to 2000, he was a Postdoctoral Researcher at Bell Laboratories, Lucent Technologies, Murray Hill, NJ, working on integrated photonic circuits for ultrafast switching applications. In 2000, he joined the Advanced Technology Department of Siemens Information and Communication Networks (ICN), Munich, Germany. He initiated and managed the IST project FASHION, was leading the Advanced Technology optical networking group, and was responsible for the advanced optical link design activities at Siemens ICN. In 2004, he took over new responsibilities in the DWDM system development.

G.-D. Khoe (S'71–M'71–SM'85–F'91) was born in Magelang, Indonesia, on July 22, 1946. He received the Elektrotechnisch Ingenieur degree (*cum laude*) from Eindhoven University of Technology, Eindhoven, The Netherlands, in 1971.

In 1971, he started his research career at the Dutch Foundation for Fundamental Research on Matter (FOM) Laboratory on Plasma Physics, Rijnhuizen, The Netherlands. In 1973, he joined the Philips Research Laboratories, Eindhoven, The Netherlands, to conduct research in the area of optical fiber communication systems. In 1983, he was appointed as a Part Time Professor at Eindhoven University of Technology, where he became a Full Professor in 1994. Currently, he is the Chairman of the Department of Telecommunication Technology and Electromagnetics (TTE), Eindhoven University of Technology. Most of his work has been devoted to single-mode fiber systems and components. Currently, his research programs include ultrafast all-optical signal processing, high-capacity transport systems, and systems in the environment of the users. He is the author or coauthor of more than 100 papers, invited papers, and chapters in books. He is the holder of more than 40 U.S. patents.

Prof. Khoe was general Co-Chair of the European Conference on Optical Communication (ECOC) in 2001 and was a founder of the IEEE Lasers and Electro-Optics Society (LEOS) Benelux Chapter. He received the Micro-Optics Conference/Gradient Index Optical Systems (MOC/GRIN) Award in 1997. In 2003, he was appointed the President of LEOS.

H. de Waardt was born in Voorburg, The Netherlands, in December 1953. He received the M.Sc.E.E. and Ph.D. degrees from Delft University of Technology, Delft, The Netherlands, in 1980 and 1995, respectively, both in electrical engineering.

In 1981, he joined the Physics Department, PTT Research, Leidschendam, The Netherlands, where he worked on performance issues of opto-electronic devices. In 1989, he moved to the Transmission Department and became involved in WDM high-bit-rate optical transmission. In 1995, he joined Eindhoven University of Technology (TU/e), Eindhoven, The Netherlands, as an Associate Professor, working on high-capacity trunk transmission. He coordinated the participation of TU/e in ACTS Upgrade, ACTS BLISS, ACTS APEX, and IST FASHION. Currently, he has been working as a Project Leader of the National Research Initiative Freeband Broadband Photonics (2004–2008). He is the coauthor of more than 100 conference and journal papers. His current interests include high-capacity optical transmission and networking, integrated optics, and semiconductor optical amplifiers.

Dr. de Waardt is a member of the IEEE Lasers and Electro-Optics Society.